Inverse Problems

PAPER

A regularized weighted least gradient problem for conductivity imaging

To cite this article: A Tamasan and A Timonov 2019 *Inverse Problems* **35** 045006

IOP Publishing　　Inverse Problems

Inverse Problems **35** (2019) 045006 (20pp)　　https://doi.org/10.1088/1361-6420/aaf2fd

A regularized weighted least gradient problem for conductivity imaging

A Tamasan[1] **and A Timonov**[2]

[1] Department of Mathematics, University of Central Florida, Orlando, FL, United States of America

[2] Division of Mathematics and Computer Science, University of South Carolina Upstate, Spartanburg, SC, United States of America

E-mail: tamasan@math.ucf.edu and atimonov@uscupstate.edu

Received 2 April 2018, revised 5 November 2018
Accepted for publication 22 November 2018
Published 5 March 2019

Abstract

We propose and study a method for imaging an approximate electrical conductivity from the magnitude of one interior current density field without any knowledge of the boundary voltage potential. Solely from this interior data, the exact conductivity is impossible to recover as non-unique solutions exist. We propose a method to recover a minimum residual type solution. The method is based on a weighted least gradient problem in the subspace of functions of bounded variations with square integrable traces. We prove existence and uniqueness for a nearby problem, and study the continuous dependence data for a regularized problem. The computational effectiveness and numerical convergence of this method is demonstrated in numerical experiments.

Keywords: minimum weighted gradient, conductivity imaging, current density impedance imaging, generalized 1-Laplacian

1. Introduction

Let $\Omega \subset R^d$, $d = 2, 3$, be a Lipschitz domain modeling a conductive body. We revisit the inverse hybrid problem of reconstructing an inhomogeneous, isotropic, electrical conductivity σ from knowledge of the magnitude of one current density field inside Ω. The problem may be reduced to solving a singular, degenerate elliptic equation (the 1-Laplacian in a conformal Euclidean metric) subject to various boundary conditions [12, 22], or can be cast as a minimization problem involving a weighted gradient term [19, 23, 26]. Without some minimal knowledge of the voltage potential at the boundary, the problem has non-unique solution as recently characterized in [26], where additional measurements of the voltage potential along a curve joining the electrodes were proposed to establish uniqueness. Other approaches, some of which are mentioned below, assume knowledge of the magnitude of two current density fields, or of the entire field. To date, the only known modality of obtaining the interior data involves rotations in a magnetic resonance machine [30]. This makes any boundary voltage potential measurement, while not impossible, at least impractical.

The forward problem is modeled by the Robin boundary conditions as follows. Assume that a current density field is generated by injecting/extracting a net current $I > 0$ from a couple of surface electrodes $e_\pm$ assumed bounded Lipschitz subdomains in $\partial\Omega$, with real valued impedance $z > 0$. For a known conductivity σ, the voltage potential $u_0 \in H^1(\Omega)$ (functions and their gradient are square integrable) distributes inside according to

$$\nabla \cdot \sigma \nabla u_0 = 0, \quad \text{in } \Omega, \tag{1}$$

$$\sigma \frac{\partial u_0}{\partial \nu} = -b_0 u_0 + c_0, \quad \text{on } \partial\Omega, \tag{2}$$

where

$$b_0 := \begin{cases} 1/z \text{ on } e_\pm, \\ 0, \text{ off } e_\pm, \end{cases} \qquad \text{and} \qquad c_0 := \begin{cases} \pm I, \text{ on } e_\pm, \\ 0, \text{ off } e_\pm, \end{cases} \tag{3}$$

and ν denotes the outer unit normal to the boundary,

By replacing the conductivity in (1) by $a/|\nabla u_0|$, the problem reduces to solving a boundary value problem for a generalized 1-Laplacian as originally proposed in [12]. The work in [22] was first to point out the connection with minimum surfaces in a Riemannian space determined by the interior data, and proposed a method to recover the conductivity from Cauchy data. For Dirichlet data in [23, 24] the problem was reduced to minimum gradient problem for functions of given trace at the boundary, and, in [26], extended to the complete electrode model (CEM) boundary conditions originally introduced in [31]. Existence and/or uniqueness of such weighted gradient problems were studied in [8] and [21], with extensions to perfectly insulated and conducting inclusions in [20, 21]. A structural stability result for the minimization problem can be found in [27]. Reconstruction algorithms based on the minimization problem were proposed in [23] and [19], and based on level set methods in [22, 23, 33]. Continuous dependence on σ on a (for a given unperturbed Dirichlet data) can be found in [17], and, for partial data in [18]. For further references on determining the isotropic conductivity based on measurements of current densities see [11–16, 25, 32, 35], and for reconstructions on anisotropic conductivities from multiple measurements see [2, 3, 7, 10].

In here we seek to determine an approximate conductivity σ, from knowledge of the magnitude of the current density field,

$$a_0 := |\sigma \nabla u_0|, \tag{4}$$

where $u_0 \in H^1(\Omega)$ is the unique solution to the Robin problem (1) and (2). The impedance of the surface electrodes $z > 0$, and the injected amperage $I > 0$ are assumed known.

As characterized in [26], we note that σ is not uniquely determined by a_0. For example, for any $\varphi : \text{Range}(u_0) \to \text{Range}(u_0)$ an increasing Lipschitz continuous function, satisfying $\varphi(t) = t$ for $t \in u_0(e_+) \cup u_0(e_-)$, one can verify that $u_\varphi = \varphi \circ u_0$ is another solution of the Robin problem corresponding to the conductivity $\sigma/(\varphi' \circ u_0)$, while the magnitude of the induces current density field does not change. We address the issue of non-uniqueness via a regularization method that recovers an approximate conductivity without recourse to any boundary voltage information. In any vicinity of the given interior data we identify the virtual data that uniquely determines the sought conductivity. The given data is considered as a perturbation of the virtual data. In accordance with the theory of ill-posed problems (see, e.g.

[1]), the regularization consists of selecting an element of a minimizing sequence, so that the norm of the residual does not exceed the prescribed level of perturbation. The feasibility of the proposed method is demonstrated in numerical experiments.

Similar to the original idea in [23], we approach the inverse problem via a weighted minimum gradient problem, here modeled for Robin boundary conditions. Let us introduce the functional

$$v \mapsto G(v; a, b, h) := \int_\Omega a|\nabla v|\mathrm{d}x + \frac{1}{2}\int_{\partial\Omega} b(v-h)^2 \mathrm{d}s, \tag{5}$$

defined for some nonnegative $a \in C(\Omega) \cap L^\infty(\Omega)$ (either the interior data or one of its approximations), and some boundary functions $b \in L^\infty(\partial\Omega)$ and $h \in L^1(\partial\Omega)$ arising in the Robin condition.

The smallest subspace in which a minimizing sequence of (5) is compact is the subspace $BV_2(\Omega)$ of functions of bounded variation with square integrable traces. In this regard, $|\nabla v|\mathrm{d}x$ in the first integral term is understood as a Radon measure applied to the bounded continuous function a,

$$|Dv|(a) := \sup\{\int_\Omega v\nabla \cdot F\mathrm{d}x : \ F \in C_0^1(\Omega; R^d), \ |F(x)| \leqslant a(x)\}. \tag{6}$$

In general, the minimization of the functional (5) is an open problem. However, in our inverse problem here, there is a compatibility relation between the coefficients a and (b, h) coming from the forward Robin problem. We exploit this compatibility to prove existence of a minimizer for the functional in (5). We show that the solution u_0 of the forward problem minimizes the functional $v \mapsto G(v; a_0, b_0, h_0)$ in (5) with $a = a_0$ in (4), $b = b_0$ and $h = c_0/b_0$ specified on $e_\pm$ in (3). However, it is not unique. For example, for φ as in the counterexample above, one can check that $\varphi \circ u_0$ will also be a minimizer.

The new idea idea is to find a family of triples $(a_\epsilon, b_\epsilon, h_\epsilon)$ converging to (a_0, b_0, h_0) as $\epsilon \to 0$, and such that the corresponding minimization problem for the functional $v \mapsto G(v; a_\epsilon, b_\epsilon, h_\epsilon)$ over $BV_2(\Omega)$ has the unique minimizer $u_\epsilon \in H^1(\Omega)$; see theorem 1. This property, that

$$\exists! \ \mathrm{argmin}\{G(v; \ a_\epsilon, b_\epsilon, c_\epsilon, h), : \ v \in BV_2(\Omega)\} \in H^1(\Omega), \tag{7}$$

is key in proving convergence of a minimizing (sub)sequence in section 5, and in devising the algorithm in section 7. Note that u_ϵ is also the voltage potential corresponding to a Robin problem for the same conductivity σ.

While b_ϵ, h_ϵ are explicit in terms of b_0 and h_0, the construction of a_ϵ is implicit (depends on the unknown σ). We are thus forced to consider the minimization problem for $v \mapsto G(v; a_0, b_\epsilon, h_\epsilon)$, where a_0 is seen as a perturbation of a_ϵ. In general, the functional $v \mapsto G(v; a_0, b_\epsilon, h_\epsilon)$ for some fixed $\epsilon > 0$ may not have a minimizer, even in $BV_2(\Omega)$. This motivates to work with the regularized functional

$$v \mapsto G^\delta(v; a, b_\epsilon, h_\epsilon) := G(v; a, b_\epsilon, h_\epsilon) + \frac{\delta}{2}\int_\Omega |\nabla(v - h_\epsilon)|^2 \mathrm{d}x, \tag{8}$$

where h_ϵ is now an arbitrary $H^1(\Omega)$-extension from the boundary inside, and $\delta > 0$.

We consider the data dependence problem for G^δ with respect to a and δ, and prove the compactness of a minimizing sequence as $a \to a_\epsilon$ and $\delta \to 0$, see theorem 2. This result depends crucially on the fact that $G(v; a, b_\epsilon, h_\epsilon)$ when $a = a_\epsilon$ satisfies (7), and is independent of the choice of the extension of h_ϵ.

We propose an iterative algorithm, where at each step the functional is strictly minimized, see theorem 3. For this result we use the harmonic extension of h_ϵ as an $H^1(\Omega)$ map. The effect of this choice of the extension on the recovered conductivity is subject of further studies. However, regardless of this extension, the algorithm recovers a minimum residual solution σ_ϵ in the following sense: if $\sigma \mapsto |J|(\sigma) := \sigma|\nabla u(\sigma)|$ denotes the nonlinear operator for which a right inverse is sought, the recovered σ_ϵ is such that $\| |J|(\sigma_\epsilon) - |J|(\sigma)\|_{L^2} \leqslant \epsilon$.

To connect with the work in [26] in the appendix we remark that, for two electrodes, the Robin problem is equivalent to the complete electrode model (CEM) problem in [31] up to a scaling factor. Moreover, in the numerical experiments, the simulated data is generated by solving a forward CEM, whereas the reconstruction method is based on the Robin problem.

2. Remarks on the smoothness of solutions to the Robin problem

Our technique, which is based on the minimization of the functional (5) in a subspace of functions of bounded variation, requires the weight a (the product of σ with the magnitude of the gradient of the solution of a Robin problem) be bounded continuous in Ω. This regularity cannot be achieved solely on the smoothness in the conductivity σ, as the regularity of the coefficients appearing in the Robin condition (2) also play a role. Throughout we assume a conductivity

$$\sigma \in C^{1/2}(\overline{\Omega}) \text{ with } \sigma|_{\partial\Omega} \in C^2(\partial\Omega), \text{ and } \sigma > 0. \tag{9}$$

Under this smoothness assumption, the elliptic regularity for solutions to the Robin problem (e.g. [9, theorem 7.4 and remark 7.2]) yields that $u_0 \in C^{1/2}(\overline{\Omega}) \cap C^{1,1/2}(\Omega)$. Moreover, ∇u_0 and thus a_0 in (4) extend by Hölder-continuity to all points in $\partial\Omega \setminus \partial e_\pm$, see [26, proposition B.1. (ii)] for details. By itself, this regularity is insufficient to yield boundedness of $|\nabla u_0|$ at points on the boundary $\partial e_\pm$ of the electrodes.

In our case, the jump in the coefficients b_0 and c_0, yield the right hand side of (2) be merely in $H^{\frac{1}{2}-s}$ for some $s > 0$. Then u_0 is merely in $H^{3-s}(\Omega)$, which is insufficient to conclude the boundedness of ∇u_0 in three dimensions. Namely, at the boundary of the electrodes, the tangential derivative normal to $\partial e_\pm$ may blow up, yielding an unbounded interior data a_0 in (4). However, if $b_\epsilon, c_\epsilon \in H^{3/2}(\partial\Omega)$ are smooth approximations of b_0 and c_0, then the bootstrap argument in the proof of [26, proposition B.1. (ii)] applies to yield that the corresponding Robin problem has a solution $u_\epsilon \in H^3(\Omega)$: indeed, for a right hand side of (2) in $H^{1/2}(\partial\Omega)$, the solution $u_\epsilon \in H^2(\Omega)$, which in turn yields $u_\epsilon \in H^{3/2}(\partial\Omega)$. Since $b_\epsilon, c_\epsilon \in H^{3/2}(\partial\Omega)$, we get $u_\epsilon b_\epsilon \in H^{3/2}(\partial\Omega)$ and thus that the right hand side of (2) now lie in $H^{3/2}(\partial\Omega)$. Another application of the classical regularity result yields $u_\epsilon \in H^3(\Omega) \subset C^{1,1/2}(\overline{\Omega})$. Therefore in two and three dimensions, $a_\epsilon := \sigma|\nabla u_\epsilon| \in C^{1/2}(\overline{\Omega})$ is bounded continuous.

3. Existence and uniqueness of a minimizer in $BV_2(\Omega)$ for a nearby problem

The regularized method can be understood through a family of forward problems. Recall the coefficients b_0 and c_0 in (3), and for each $\epsilon > 0$ small, let first define the piecewise boundary function

$$\tilde{b}_\epsilon := \begin{cases} 1/z \text{ on } e_\pm, \\ \epsilon/z, \text{ on } \partial\Omega \setminus (e_- \cup e_+). \end{cases}$$

According to the regularity remarks above, the solution to the problem (1) subject to the Robin boundary condition

$$\sigma \frac{\partial u}{\partial \nu} = -\tilde{b}_\epsilon u + c_0, \quad \text{on } \partial\Omega,$$

might not be of bounded gradient (regularity needed in order for $a = |\sigma \nabla u|$ to be bounded continuous).

This motivates to further consider some smooth approximates $b_\epsilon \in H^{3/2}(\partial\Omega)$ of $\tilde{b}_\epsilon$, and $c_\epsilon \in H^{3/2}(\partial\Omega)$ of c_0, with the only necessary property that

$$\lim_{\epsilon\to 0} \|b_\epsilon - b_0\|_\infty = 0, \text{ and } \lim_{\epsilon\to 0} \|c_\epsilon - c_0\|_\infty = 0. \tag{10}$$

Let $u_\epsilon \in H^1(\Omega)$ be the solution of the Robin problem (1) subject to

$$\sigma \frac{\partial u}{\partial \nu} = -b_\epsilon u + c_\epsilon, \quad \text{on } \partial\Omega, \tag{11}$$

and define an 'ideal' interior coefficient a_ϵ as the magnitude of the corresponding current density field,

$$a_\epsilon := |\sigma \nabla u_\epsilon|. \tag{12}$$

The remarks of section 2 show that $a_\epsilon \in C^{1/2}(\overline{\Omega})$ for $\epsilon > 0$.

Classical arguments on the continuous dependence (in particular, since the coercivity constant is bounded below independently of ϵ), also apply to yield

$$\|u_\epsilon - u_0\|_{H^1(\Omega)} \to 0, \text{ and } \|a_\epsilon - a_0\|_{L^2(\Omega)} \to 0, \text{ as } \epsilon \to 0^+.$$

Also for $\epsilon > 0$, let h_ϵ be defined at the boundary $\partial\Omega$ by

$$h_\epsilon := \frac{c_\epsilon}{b_\epsilon}. \tag{13}$$

For uniformity, let also define $h_0 \in L^\infty(\partial\Omega)$ on the electrodes by $h_0 = c_0/b_0$, and $h_0 = 0$ off the electrodes.

Recall the functional in (5):

$$v \mapsto G(v; a, b, h) := \int_\Omega a|\nabla v| \mathrm{d}x + \frac{1}{2}\int_{\partial\Omega} b(v-h)^2 \mathrm{d}s.$$

The following result shows the regularizing effect of $\epsilon > 0$.

Theorem 1. *Let σ satisfy (9). For $\epsilon \geqslant 0$, let $a_\epsilon, b_\epsilon, h_\epsilon$, and u_ϵ be the solutions to the Robin problem (1) and (11) as defined above. Then, for $\epsilon \geqslant 0$,*

$$G(u_\epsilon; a_\epsilon, b_\epsilon, h_\epsilon) \leqslant G(v; a_\epsilon, b_\epsilon, h_\epsilon), \quad \text{for all } v \in H^1(\Omega). \tag{14}$$

Moreover, if $\epsilon > 0$, then

$$G(u_\epsilon; a_\epsilon, b_\epsilon, h_\epsilon) \leqslant G(v; a_\epsilon, b_\epsilon, h_\epsilon), \quad \text{for all } v \in BV_2(\Omega), \tag{15}$$

$u_\epsilon \in C^{1,1/2}(\overline{\Omega})$ is the unique minimizer, and the exact conductivity can be recovered from a_ϵ by

$$\sigma = \frac{a_\epsilon}{|\nabla u_\epsilon|}. \tag{16}$$

Proof. Let $\epsilon \geqslant 0$. For any $v \in H^1(\Omega)$, we estimate

$$\begin{aligned} G(v; a_\epsilon, b_\epsilon, h_\epsilon) &= \int_\Omega a_\epsilon |\nabla v| \mathrm{d}x + \frac{1}{2}\int_{\partial\Omega} b_\epsilon (v - h_\epsilon)^2 \mathrm{d}s \\ &= \int_\Omega \sigma |\nabla u_\epsilon||\nabla v| \mathrm{d}x + \frac{1}{2}\int_{\partial\Omega} b_\epsilon (v - h_\epsilon)^2 \mathrm{d}s \\ &\geqslant \int_\Omega \sigma \nabla u_\epsilon \cdot \nabla v \mathrm{d}x + \frac{1}{2}\int_{\partial\Omega} b_\epsilon (v - h_\epsilon)^2 \mathrm{d}s \\ &= \int_{\partial\Omega} (-b_\epsilon u_\epsilon + c) v \mathrm{d}s + \frac{1}{2}\int_{\partial\Omega} b_\epsilon (v - h_\epsilon)^2 \mathrm{d}s \\ &= \frac{1}{2}\int_{\partial\Omega} b_\epsilon (v - u_\epsilon)^2 \mathrm{d}s + \frac{1}{2}\int_{\partial\Omega} b_\epsilon (h_\epsilon^2 - u_\epsilon^2) \mathrm{d}s \\ &\geqslant \frac{1}{2}\int_{\partial\Omega} b_\epsilon (h_\epsilon^2 - u_\epsilon^2) \mathrm{d}s = G(u_\epsilon; a_\epsilon, b_\epsilon, h_\epsilon), \end{aligned} \tag{17}$$

where the second equality uses (12), the third equality uses the divergence theorem and the fact the u_ϵ solves the Robin problem (1) and (11). This proves (14).

Now let $\epsilon > 0$. We show first that u_ϵ is a global minimizer of the functional over the larger set $BV_2(\Omega)$. Let $v \in BV_2(\Omega)$ be arbitrary. By mollification (e.g. [6, remark 2.12]), there exists a sequence $\{v_n\} \subset H^1(\Omega)$ with $v_n|_{\partial\Omega} = v|_{\partial\Omega}$ (as traces in $L^1(\partial\Omega)$), and such that $v_n \to v$ in $L^1(\Omega)$, and

$$\lim_{n\to\infty} \int_\Omega a_\epsilon |\nabla v_n| \mathrm{d}x = |Dv|(a_\epsilon). \tag{18}$$

Since (14) now holds,

$$\begin{aligned} G_\epsilon(u_\epsilon; a_\epsilon, b_\epsilon, h_\epsilon) &\leqslant G_\epsilon(v_n; a_\epsilon, b_\epsilon, h_\epsilon) \\ &= \int_\Omega a_\epsilon |\nabla v_n| \mathrm{d}x + \int_{\partial\Omega} b_\epsilon (v - h_\epsilon)^2 \mathrm{d}s, \end{aligned} \tag{19}$$

where the equality above uses the fact that $v_n|_{\partial\Omega} = v|_{\partial\Omega}$. By taking the limit with $n \to \infty$ in (19), and using (18), we conclude that

$$G_\epsilon(u_\epsilon; a_\epsilon, b_\epsilon, h_\epsilon) \leqslant |Dv|(a_\epsilon) + \int_{\partial\Omega} b_\epsilon (v - h_\epsilon)^2 \mathrm{d}s = G(v; a_\epsilon, b_\epsilon, h_\epsilon).$$

Next we prove uniqueness. Let $v \in BV_2(\Omega)$ be another minimizer of $G(\cdot; a_\epsilon, b_\epsilon, h_\epsilon)$, and consider a mollified sequence $\{v_n\} \subset H^1(\Omega)$, $v_n|_{\partial\Omega} = v|_{\partial\Omega}$ as above to estimate

$$\begin{aligned}
G(v;a_\epsilon,b_\epsilon,h_\epsilon) &= |Dv|(a_\epsilon)+\frac{1}{2}\int_{\partial\Omega}b_\epsilon(v-h_\epsilon)^2\mathrm{d}s\\
&= \lim_{n\to\infty}\int_\Omega \sigma|\nabla u_\epsilon||\nabla v_n|\mathrm{d}x+\frac{1}{2}\int_{\partial\Omega}b_\epsilon(v-h_\epsilon)^2\mathrm{d}s\\
&\geqslant \limsup_{n\to\infty}\int_\Omega \sigma\nabla u_\epsilon\cdot\nabla v_n\mathrm{d}x+\frac{1}{2}\int_{\partial\Omega}b_\epsilon(v-h_\epsilon)^2\mathrm{d}s\\
&= \limsup_{n\to\infty}\int_{\partial\Omega}(-b_\epsilon u_\epsilon+c_\epsilon)v_n\mathrm{d}s+\frac{1}{2}\int_{\partial\Omega}b_\epsilon(v-h_\epsilon)^2\mathrm{d}s\\
&= \int_{\partial\Omega}(-b_\epsilon u_\epsilon+c_\epsilon)v\mathrm{d}s+\frac{1}{2}\int_{\partial\Omega}b_\epsilon(v-h_\epsilon)^2\mathrm{d}s\\
&= \frac{1}{2}\int_{\partial\Omega}b_\epsilon(v-u_\epsilon)^2\mathrm{d}s+\frac{1}{2}\int_{\partial\Omega}b_\epsilon(h_\epsilon^2-u_\epsilon^2)\mathrm{d}s\\
&\geqslant \frac{1}{2}\int_{\partial\Omega}b_\epsilon(h_\epsilon^2-u_\epsilon^2)\mathrm{d}s=G_\epsilon(u_\epsilon;a_\epsilon,b_\epsilon,h_\epsilon).
\end{aligned}$$

Since v is also a minimizer $G_\epsilon(v;a_\epsilon,b_\epsilon,h_\epsilon)=G_\epsilon(u_\epsilon;a_\epsilon,b_\epsilon,h_\epsilon)$ and all the inequalities above hold with equality, in particular

$$\int_{\partial\Omega}b_\epsilon(v-u_\epsilon)^2\mathrm{d}s=0.$$

Since the weight b_ϵ is essentially positive on the boundary, we conclude that

$$v|_{\partial\Omega}=u_\epsilon|_{\partial\Omega}. \tag{20}$$

Next, we note that, for competitors restricted to the affine subspace

$$D_\epsilon:=\{v\in BV_2(\Omega):\ v|_{\partial\Omega}=u_\epsilon|_{\partial\Omega}\},$$

the minimization problem $\min\{G_\epsilon(v;a_\epsilon,b_\epsilon,h_\epsilon):\ v\in D_\epsilon\}$ is equivalent to

$$\min\{|Dv|(a_\epsilon):v\in BV(\Omega),\ v|_{\partial\Omega}=u_\epsilon|_{\partial\Omega}\}. \tag{21}$$

Since $u_\epsilon\in C^{1,1/2}(\overline{\Omega})$ is a solution, we apply the uniqueness result [21, theorem 1.1] to the minimization problem (21) to conclude that

$$v=u_\epsilon,\quad \text{in }\Omega.$$

Following from the definition of a_ϵ in (12), and the strict positivity of the conductivity, the set of critical points $\{x\in\Omega:\ |\nabla u_\epsilon|=0\}$ coincide with the set of zeros of a_ϵ. Since u_ϵ is a solution of an elliptic equation. The set of critical points is negligible in Ω, the equality (16) holds almost everywhere. Since σ is assumed continuous, the equality (16) must then hold at all points in Ω.

□

We stress here that, for $\epsilon>0$, the uniqueness of the minimizer is not a consequence of the classical methods in the theory of augmented Lagrangian, e.g., in [5], but rather of the uniqueness result in [21].

4. Regularization of the weighted least gradient problem

The results of theorem 1 cannot apply directly to recover σ: on the one hand, for $\epsilon=0$, the minimizer u_0 is not unique, on the other hand for $\epsilon>0$, we are not given the coefficient a_ϵ, but rather its approximate a_0, and the existence pf minimizers for $v\mapsto G(v;a_0,b_\epsilon,a_\epsilon)$ is not clear in general. This motivates to consider the regularized functional $v \mapsto G^{\delta}(v; a, b, h)$ in (8) and study the continuous dependence of its minimizer with respect to a and δ.

To simplify notation, since b and h are fixed, we drop the explicit dependence in the notation of the functional G^{δ} and work with

$$G^{\delta}(v; a) := \int_{\Omega} a|\nabla v|\mathrm{d}x + \int_{\partial\Omega} b(v-h)^2\mathrm{d}s + \frac{\delta}{2}\int_{\Omega} |\nabla(v-h)|^2\mathrm{d}x. \tag{22}$$

In this section we assume that $a \in L^2(\Omega)$ is bounded away from zero,

$$0 < \frac{\epsilon}{z} \leqslant b \leqslant \frac{1}{z}, \text{ a.e. } \partial\Omega, \tag{23}$$

while $h \in H^1(\Omega)$ is arbitrarily fixed.

The sum

$$F^{\delta}(v) := \frac{1}{2}\int_{\partial\Omega} bv^2\mathrm{d}s + \frac{\delta}{2}\int_{\Omega} |\nabla v|^2\mathrm{d}x \tag{24}$$

of the quadratic terms in (22) defines an equivalent square norm in $H^1(\Omega)$, since

$$\min\left\{\frac{\epsilon}{2z}, \frac{\delta}{2}\right\}\|u\|_1^2 \leqslant F^{\delta}(u) \leqslant \max\left\{\frac{1}{2z}, \frac{\delta}{2}\right\}\|u\|_1^2, \tag{25}$$

where

$$\|u\|_1^2 := \int_{\partial\Omega} |u|^2\mathrm{d}s + \int_{\Omega} |\nabla u|^2\mathrm{d}x.$$

Existence and uniqueness of the minimizer in $H^1(\Omega)$ of the functional (22) follows from classical convex minimization arguments, recalled below for completeness.

Proposition 1. *For $\epsilon, \delta > 0$ arbitrarily fixed, and $a \in L^2(\Omega)$ positive, let $G^{\delta}(\cdot, a)$ be the functional in (22). The minimization problem*

$$\min\{G^{\delta}(v; a) : \ v \in H^1(\Omega)\}$$

has a unique solution.

Proof. We show first that $G^{\delta}(\cdot; a)$ is weakly lower semi-continuous. Let $v_n \rightharpoonup v$ be a weakly convergent sequence in $H^1(\Omega)$. We need to show that

$$G^{\delta}(v; a) \leqslant \liminf_{n\to\infty} G^{\delta}(v_n; a). \tag{26}$$

The weak lower semicontinuity of $F_{\epsilon}^{\delta} : H^1(\Omega) \to R$ follows from its convexity

$$F_{\epsilon}^{\delta}(v_n) \geqslant F_{\epsilon}^{\delta}(v) + \int_{\partial\Omega} b_{\epsilon}v(v_n - v)\mathrm{d}s + \delta\int_{\Omega} \nabla v \cdot \nabla(v_n - v)\mathrm{d}x,$$

and Fatou's lemma. The weak lower semicontinuity of the weighted gradient functional

$$v \mapsto \int_{\partial\Omega} a|\nabla v|\mathrm{d}x \tag{27}$$

also follows from standard arguments: let $\{a_m\}$ be an increasing sequence of bounded continuous functions, which converges in $L^2(\Omega)$ sense to a. For each fixed index m, let $f \in C_0^1(\Omega; R^d)$

be arbitrary with $|f| \leqslant a_m$. Since $v_n \rightharpoonup v$ in $L^2(\Omega)$ we have

$$\int_\Omega v\nabla\cdot f\mathrm{d}x = \lim_{n\to\infty}\int_\Omega v_n\nabla\cdot f\mathrm{d}x = \liminf_{n\to\infty}\int_\Omega v_n\nabla\cdot f\mathrm{d}x$$
$$\leqslant \liminf_{n\to\infty}\ \sup\left\{\int_\Omega v_n\nabla\cdot g\mathrm{d}x:\ g\in C_0^1(\Omega;R^n),\ |g|\leqslant a_m\right\}$$
$$= \liminf_{n\to\infty}\int_\Omega a_m|\nabla v_n|\mathrm{d}x \leqslant \liminf_{n\to\infty}\int_\Omega a|\nabla v_n|\mathrm{d}x, \tag{28}$$

where the last inequality above uses the fact that $a_m \leqslant a$. By taking the supremum in (28) over all $f\in C_0^1(\Omega;R^d)$ with $|f|\leqslant a_m$ we get

$$\int_\Omega a_m|\nabla v|\mathrm{d}x = \sup\left\{\int_\Omega v\nabla\cdot f\mathrm{d}x:\ f\in C_0^1(\Omega;R^d),\ |f|\leqslant a_m\right\}$$
$$\leqslant \liminf_{n\to\infty}\int_\Omega a_0|\nabla v_n|\mathrm{d}x. \tag{29}$$

By letting $m\to\infty$ in (29) we obtain the weakly lower semi-continuity for (27).

Therefore $v\mapsto G^\delta(v;a): H^1(\Omega)\to R$ is weakly lower semi-continuous in $H^1(\Omega)$. Since the $G^\delta(\cdot;a)$ is also strictly convex (as a sum of a convex with a strictly convex), it has a unique minimizer. □

In is worth noting that if, for some fixed $\epsilon>0$, the functional $v\mapsto G(v;a_0,b_\epsilon,h_\epsilon)$ has a $C^1(\Omega)$-minimizer then the uniqueness part of the proof of theorem 1 yields that it would be unique among all minimizers in $BV_2(\Omega)$. As a consequence any minimization algorithm for $G^\delta(\cdot;a_0,b_\epsilon,h_\epsilon)$ with $\delta\to 0^+$ would produce that unique solution, regardless of the choice of the $H^1(\Omega)$-extension of h_ϵ.

5. Compactness of the regularized minimizing sequence

In this section we assume $a\in C(\Omega)\cap L^\infty(\Omega)$,

$$\inf(a) =: \alpha > 0, \tag{30}$$

$b\in L^\infty(\partial\Omega)$ with

$$0<\frac{\epsilon}{z}\leqslant b\leqslant\frac{1}{z},\ \text{a.e. }\partial\Omega, \tag{31}$$

and $h\in H^1(\Omega)$ arbitrarily fixed.

Recall the functional $v\mapsto G(v;a,b,h)$ in (5). Similar to the notation in (22), since b and h will be fixed, we drop the dependence from the notation and work with

$$G(v;a) := \int_\Omega a|\nabla v|\mathrm{d}x + \int_{\partial\Omega} b(v-h)^2. \tag{32}$$

If $v\in BV_2(\Omega)$, then the first integral is understood as a Radon measure applied to a.

We assume that $v\mapsto G(v;a)$ satisfies the existence and uniqueness hypothesis (7), i.e. there is some $u\in H^1(\Omega)$, such that

$$G(u;a)\leqslant G(v;a),\quad \forall v\in BV_2(\Omega), \tag{33}$$

and u is the unique minimizer in $BV_2(\Omega)$.

We will often use the trivial identity

$$\int_\Omega \tilde{a}|\nabla v|\mathrm{d}x = \int_\Omega a|\nabla v|\mathrm{d}x + \int_\Omega (\tilde{a}-a)|\nabla v|\mathrm{d}x, \tag{34}$$

which allows us to exchange two arbitrary weights $a, \tilde{a} \in L^2(\Omega)$. By $\|\cdot\|$ we denote the $L^2(\Omega)$-norm, and by $\|\cdot\|_1$ the $H^1(\Omega)$-norm.

The following result provides the theoretical basis of our reconstruction method.

Theorem 2. *Let $\Omega \subset R^d$ be a bounded Lipschitz domain with connected boundary, and $a \in C(\Omega) \cap L^\infty(\Omega)$ satisfy (30). Assume that the functional $G(\cdot; a)$ in (32) satisfy the hypothesis (7), and let $u \in H^1(\Omega)$ be the unique minimizer*

$$u = \operatorname{argmin}\{G(v; a) : \ v \in BV_2(\Omega)\}. \tag{35}$$

Let $\{a_n\} \subset L^2(\Omega)$ be a sequence of positive functions, with

$$\|a_n - a\| \longrightarrow 0, \ \text{as } n \to \infty \tag{36}$$

and $\delta_n \downarrow 0$ be a decreasing sequence such that

$$\lim_{n\to\infty} \frac{\|a_n - a\|^2}{\delta_n} = 0. \tag{37}$$

Corresponding to each n, consider the regularized functional $v \mapsto G^{\delta_n}(v, a_n)$ as in (22), and let

$$u_n := \operatorname{argmin}\{G^{\delta_n}(v, a_n) : \ v \in H^1(\Omega)\} \tag{38}$$

be the corresponding minimizer provided by proposition 1. Then

$$\lim_{n\to\infty} G^{\delta_n}(u_n; a_n) = \lim_{n\to\infty} G(u_n; a) = G(u; a). \tag{39}$$

Moreover, on a subsequence $\{\tilde{u}_n\}$ of $\{u_n\}$,

$$\tilde{u}_n \longrightarrow u, \ \text{in } L^q(\Omega), \ 0 \leqslant q \leqslant \frac{d}{d-1},$$

and, for any open subset $O \subset \Omega$,

$$\lim_{n\to\infty} \int_O a_n|\nabla \tilde{u}_n|\mathrm{d}x = \lim_{n\to\infty} \int_O a|\nabla \tilde{u}_n|\mathrm{d}x = \int_O a|\nabla u|\mathrm{d}x. \tag{40}$$

Proof. Despite the fact that $\|u_n\|_1$ may not be uniformly bounded, we prove first that

$$\lim_{n\to\infty} \int_\Omega (a - a_n)|\nabla u_n|\mathrm{d}x = 0. \tag{41}$$

Let n be sufficiently large so that $\|a_n\| \leqslant 2\|a\|$. Recall the functional $F^{\delta_n}(\cdot; a_n)$ in (24) with $\delta = \delta_n$ and $a = a_n$, and the induced norm on $H^1(\Omega)$ in (25). We estimate

$$\begin{aligned}\min\left\{\frac{\epsilon}{2z},\frac{\delta_n}{2}\right\}\|u_n-h\|_1^2 &\leqslant F^{\delta_n}(u_n-h;a_n)\\ &\leqslant F^{\delta_n}(u_n-h;a_n)+\int_\Omega a_n|\nabla u_n|\mathrm{d}x\\ &= G^{\delta_n}(u_n;a_n)\\ &\leqslant G^{\delta_n}(h;a_n)\\ &= \int_\Omega a_n|\nabla h|\mathrm{d}x\\ &\leqslant 2\|a\|\|\nabla h\|,\end{aligned} \tag{42}$$

where the third inequality uses the minimizing property defining u_n. Note that the right hand side of (42) is independent of δ_n to yield

$$\|u_n\|_1 \leqslant C\max\left\{\frac{2z}{\epsilon},\frac{2}{\delta_n}\right\}^{1/2}, \tag{43}$$

for some constant C dependent on $\|a\|$ and $\|h\|_1$. In particular since $\delta_n\to 0$, for sufficiently large n, we obtained

$$\|u_n\|_1 \leqslant C\frac{1}{\sqrt{\delta_n}}, \tag{44}$$

where C depends only on $\|a\|$ and the $\|h\|_1$. The rate of decay (37) together with (44) yields (41). □

Since u is a minimizer of $G(\cdot;a)$, we estimate

$$\begin{aligned}G(u;a) &\leqslant \liminf_{n\to\infty} G(u_n;a) \leqslant \limsup_{n\to\infty} G(u_n;a)\\ &= \limsup_{n\to\infty}\left\{G(u_n;a_n)+\int_\Omega(a-a_n)|\nabla u_n|\mathrm{d}x\right\}\\ &\leqslant \limsup_{n\to\infty}\left\{G(u_n;a_n)+\frac{\delta_n}{2}\int_\Omega|\nabla(u_n-h)|^2\mathrm{d}x+\int_\Omega(a-a_n)|\nabla u_n|\mathrm{d}x\right\}\\ &= \limsup_{n\to\infty}\left\{G^{\delta_n}(u_n;a_n)+\int_\Omega(a-a_n)|\nabla u_n|\mathrm{d}x\right\}\\ &= \limsup_{n\to\infty} G^{\delta_n}(u_n;a_n)\end{aligned} \tag{45}$$

where the first equality uses (34), the next to the last equality uses the definition of $G_\epsilon^{\delta_n}$, and the last equality uses (41). Similarly,

$$\begin{aligned}G(u;a) &\leqslant \liminf_{n\to\infty} G(u_n;a)\\ &= \liminf_{n\to\infty}\left\{G(u_n;a_n)+\int_\Omega(a-a_n)|\nabla u_n|\mathrm{d}x\right\}\\ &\leqslant \liminf_{n\to\infty}\left\{G(u_n;a_n)+\frac{\delta_n}{2}\int_\Omega|\nabla(u_n-h)|^2\mathrm{d}x+\int_\Omega(a-a_n)|\nabla u_n|\mathrm{d}x\right\}\\ &= \liminf_{n\to\infty}\left\{G^{\delta_n}(u_n;a_n)+\int_\Omega(a-a_n)|\nabla u_n|\mathrm{d}x\right\}\\ &= \liminf_{n\to\infty} G^{\delta_n}(u_n;a_n) \leqslant \liminf_{n\to\infty} G^{\delta_n}(u_n;a_n).\end{aligned} \tag{46}$$

The reverse inequality also holds:

$$\begin{aligned}&\limsup_{n\to\infty} G^{\delta_n}(u_n;a_n) \leqslant \limsup_{n\to\infty} G^{\delta_n}(u;a_n)\\&=\limsup_{n\to\infty}\left\{G^{\delta_n}(u;a)+\int_\Omega (a_n-a)|\nabla u|\mathrm{d}x\right\}\\&=\limsup_{n\to\infty}\left\{G(u;a)+\frac{\delta_n}{2}\int_\Omega |\nabla(u-h)|^2\mathrm{d}x+\int_\Omega (a_n-a)|\nabla u|\mathrm{d}x\right\}\\&=G(u;a).\end{aligned} \tag{47}$$

In the estimate (47), the first inequality uses (38), while the last equality uses (36) and the assumption $u\in H^1(\Omega)$.

The inequalities (45)–(47) prove the identity (39). In particular, we showed that

$$\lim_{n\to\infty}\left(\int_\Omega a|\nabla u_n|\mathrm{d}x+\int_{\partial\Omega} b(u_n-h)^2\mathrm{d}s\right)=\int_\Omega a|\nabla u|\mathrm{d}x+\int_{\partial\Omega} b(u-h)^2\mathrm{d}s. \tag{48}$$

Note that both the regularization parameter and the coefficients in the functional are changing with n. In particular, the sequence u_n may not be bounded in $H^1(\Omega)$. However, we show next that $\{u_n\}$ is bounded in $W^{1,1}(\Omega)$; endowed with the norm

$$\|u\|_{1,1}:=\int_{\partial\Omega} u\mathrm{d}s+\int_\Omega |\nabla u|\mathrm{d}x.$$

Recall the lower bound α in (30) to estimate

$$\begin{aligned}&\min\{\alpha,2\sqrt{b}\}\|u_n\|_{1,1}\leqslant \int_\Omega a|\nabla u_n|\mathrm{d}x+\int_{\partial\Omega}2\sqrt{b}|u_n|\mathrm{d}s\\&\leqslant \int_\Omega a|\nabla u_n|\mathrm{d}x+\int_{\partial\Omega}2\sqrt{b_\epsilon}|u_n-h|\mathrm{d}s+\int_{\partial\Omega}2\sqrt{b}|h|\mathrm{d}s\\&\leqslant \int_\Omega a|\nabla u_n|\mathrm{d}x+\int_{\partial\Omega}b_\epsilon(u_n-h)^2\mathrm{d}s+|\partial\Omega|+\int_{\partial\Omega}2\sqrt{b}|h|\mathrm{d}s\\&\leqslant G(u_n;a)+|\partial\Omega|+\int_{\partial\Omega}2\sqrt{b}|h|\mathrm{d}s\\&=G(u_n;a_n)+\int_\Omega(a-a_n)|\nabla u_n|\mathrm{d}x+|\partial\Omega|+\int_{\partial\Omega}2\sqrt{b}|h|\mathrm{d}s\\&\leqslant G(h;a_n)+C\frac{\|a-a_n\|}{\sqrt{\delta_n}}+|\partial\Omega|+\int_{\partial\Omega}2\sqrt{b}|h|\mathrm{d}s\\&=G(h;a)+\int_\Omega(a_n-a)|\nabla h|\mathrm{d}x+C\frac{\|a-a_n\|}{\sqrt{\delta_n}}+|\partial\Omega|+\int_{\partial\Omega}2\sqrt{b}|h|\mathrm{d}s\\&=G(h;a)+\|a_n-a\|\|\nabla h\|+C\frac{\|a-a_n\|}{\sqrt{\delta_n}}+|\partial\Omega|+\int_{\partial\Omega}2\sqrt{b}|h|\mathrm{d}s,\end{aligned} \tag{49}$$

where the fifth inequality uses the bound (44). By the hypothesis (37) on the rate of decay of δ_n, the right hand side above is uniformly bounded in n.

Since $\min\{\alpha,\ \mathrm{essinf}(b)\}>0$ we showed that $\|u_n\|_{1,1}$ is uniformly bounded. An application of Rellich–Kondrachov's compactness embedding (e.g. [36]) shows the existence of a convergent subsequence $\{\tilde{u}_n\}$, with $\tilde{u}_n\to u^*$ in $L^q(\Omega)$ for all $1\leqslant q<d/(d-1)$. Moreover, since $\{\tilde{u}_n\}$ is bounded in $W^{1,1}(\Omega)$, the limit $u^*\in BV(\Omega)$ and $u^*|_{\partial\Omega}\in L^1(\partial\Omega)$, see e.g. [6].

Also following from the estimate (49), the sequence of traces $\{u_n|_{\partial\Omega}\}$ is uniformly bounded in $L^2(\partial\Omega)$. In particular, $u^*|_{\partial\Omega} \in L^2(\partial\Omega)$, and, possibly passing to a subsubsequence, $\{\tilde{u}_n\}$ converges weakly in $L^2(\partial\Omega)$ to $u^*|_{\partial\Omega}$.

We recall the weak lower semi-continuity properties on each of the two functionals in G. The first one is the lower semi-continuity of the total variations. For any $a \in C(\Omega) \cap L^\infty(\Omega)$,

$$|Du^*|(a) \leqslant \liminf_{n\to\infty} \int_\Omega a|\nabla \tilde{u}_n| \mathrm{d}x. \tag{50}$$

The second is the weak lower semi-continuity of the quadratic term,

$$\frac{1}{2}\int_{\partial\Omega} b(u^* - h)^2 \mathrm{d}s \leqslant \liminf_{n\to\infty} \frac{1}{2}\int_{\partial\Omega} b(u_n - h)^2 \mathrm{d}s. \tag{51}$$

By adding (50) and (51) and using (48) we get

$$G(u^*, a) \leqslant \liminf_{n\to\infty} G(\tilde{u}_n; a) = G(u; a). \tag{52}$$

Since u was assumed the unique minimizer of G in $BV_2(\Omega)$, we conclude that equality must hold in (52), i.e. $G(u^*; a) = \liminf_{n\to\infty} G(\tilde{u}_n; a)$, and that

$$u = u^*. \tag{53}$$

Moreover, each of the inequalities (50) and (51) must also be equalities. By possibly passing to a further sub-subsequence, we have shown that

$$\begin{aligned} |Du|(a) &= \lim_{n\to\infty} \int_\Omega a|\nabla \tilde{u}_n| \mathrm{d}x, \\ \int_{\partial\Omega} b(u - h)^2 \mathrm{d}s &= \lim_{n\to\infty} \int_{\partial\Omega} b(\tilde{u}_n - h)^2 \mathrm{d}s. \end{aligned} \tag{54}$$

For any O an open subset of Ω, the arguments of [36, theorem 5.2.3] carries verbatim to conclude the upper semi-continuity property,

$$\limsup_{n\to\infty} \int_O a|\nabla \tilde{u}_n| \mathrm{d}x \leqslant \int_O a|\nabla u| \mathrm{d}x.$$

Now (40) follows by an application of (41). □

6. The minimizing property in successive iterations

To minimize (22) we propose an iterative procedure, where at each step we solve an appropriate Robin problem for the updated conductivity. The iterative procedure is similar to those developed earlier in [23] in connection to the Dirichlet problem or in [26] in connection to the complete electrode model. A marked difference in here is due to the regularizing term, which involves an extension of the given boundary function h inside the domain. While in theorem 3 no particular extension was relevant, in the arguments below we essentially use the harmonic extension u_h:

$$\Delta u_h = 0 \text{ in } \Omega, \quad u_h = h \text{ on } \partial\Omega. \tag{55}$$

More precisely, since $\int_\Omega \nabla u_h \cdot \nabla v \mathrm{d}x = \int_{\partial\Omega} \frac{\partial u_h}{\partial \nu} v \mathrm{d}s$, one can check that

$$J^\delta(v;\sigma) = \frac{1}{2}\left\{\int_\Omega \sigma|\nabla v|^2 \mathrm{d}x + \int_{\partial\Omega} b(v-h)^2 \mathrm{d}s + \delta\int_\Omega |\nabla(v - u_h)|^2 \mathrm{d}x\right\}$$

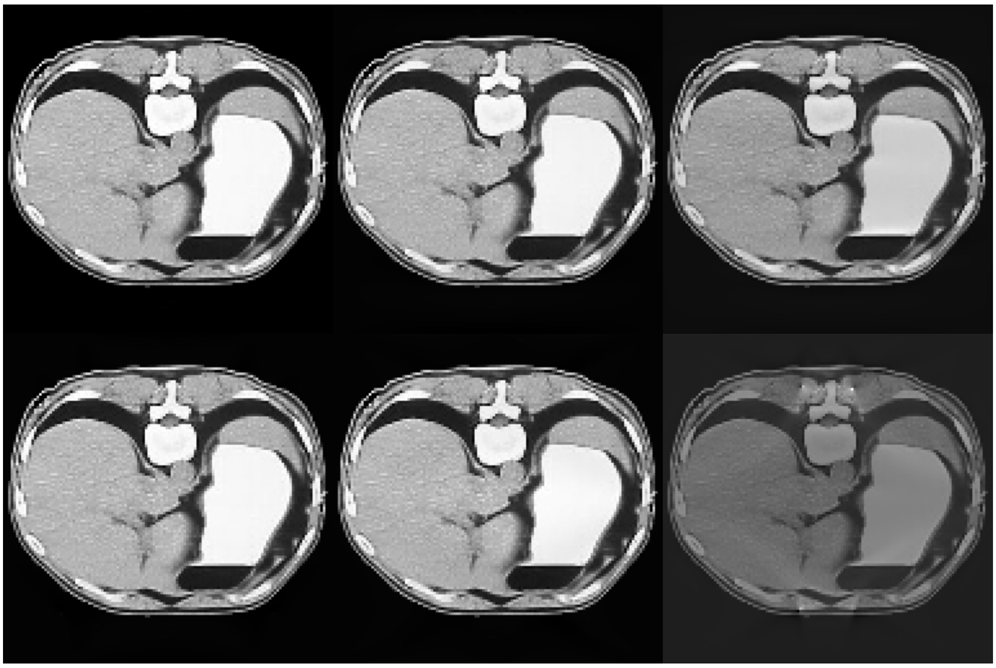

Figure 1. Comparison of the reconstructed mean conductivity distributions. The level of the roundoff and truncation errors in the interior data does not exceed 10^{-5}. The parameters $\epsilon = 5 \cdot 10^{-4}$ and $\delta = 3 \cdot 10^{-3}$ are chosen.

is the energy functional for

$$\nabla \cdot (\sigma + \delta)\nabla u = 0 \text{ in } \Omega, \tag{56}$$

$$(\sigma + \delta)\frac{\partial u}{\partial \nu} = -bu + \delta \frac{\partial u_h}{\partial \nu} \text{ on } \partial\Omega. \tag{57}$$

In particular, if $u \in H^1(\Omega)$ is the solution to (56) and (57), then

$$J^\delta(u;\sigma) \leqslant J^\delta(v;\sigma), \text{ for all } v \in H^1(\Omega). \tag{58}$$

Recall the functional G^δ in (22), which depends on the data, and contrast with J^δ above, which depends on the unknown conductivity. The minimization of G^δ algorithm by successive iterations is based on the following result.

Theorem 3. *Let $\delta > 0$, $a \in L^2(\Omega)$, and $b \in L^\infty(\partial\Omega)$ be positive. Let also $u_h \in H^1(\Omega)$ be the harmonic extension of some $h \in H^{1/2}(\partial\Omega)$ in (55). Let $v \in H^1(\Omega)$ be such that $\frac{a}{|\nabla v|} \in L^\infty(\Omega)$, and let $u \in H^1(\Omega)$ be the solution to the Robin problem*

$$\nabla \cdot \left(\frac{a}{|\nabla v|} + \delta\right) \nabla u = 0 \text{ in } \Omega, \tag{59}$$

$$\left(\frac{a}{|\nabla v|} + \delta\right) \frac{\partial u}{\partial \nu} = -bu + \delta \frac{\partial u_h}{\partial \nu} \text{ on } \partial\Omega. \tag{60}$$

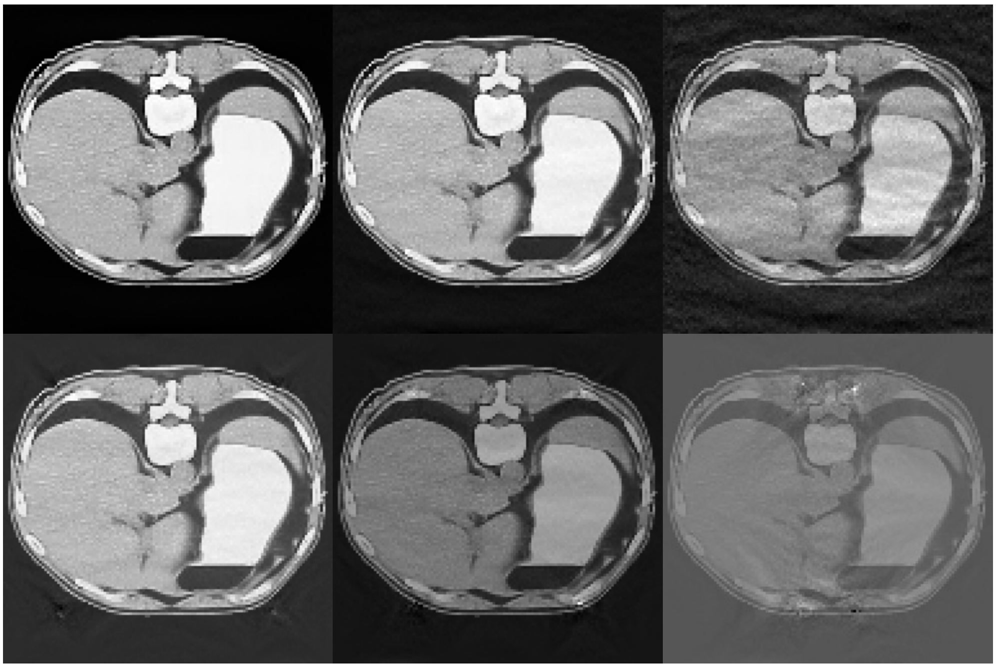

Figure 2. Comparison of the recovered conductivity from noisy interior data.

Then

$$G^{\delta}(u;a) \leqslant G^{\delta}(v;a). \tag{61}$$

Moreover, if the equality in (61) holds, then $u = v$.

Proof. On the one hand, since u is a global minimizer of $J^{\delta}(u;\sigma)$ in $H^1(\Omega)$, we obtain

$$\begin{aligned} G^{\delta}(v;a) &= \int_{\Omega} a|\nabla v|\mathrm{d}x + \frac{1}{2}\int_{\partial\Omega} b(v-h)^2\mathrm{d}s + \frac{\delta}{2}\int_{\Omega}|\nabla(v-h)|^2\mathrm{d}x \\ &= \frac{1}{2}\int_{\Omega} a|\nabla v|\mathrm{d}x + J^{\delta}\left(v;\frac{a}{|\nabla v|}\right) \\ &\geqslant \frac{1}{2}\int_{\Omega} a|\nabla v|\mathrm{d}x + J^{\delta}\left(u;\frac{a}{|\nabla v|}\right). \end{aligned} \tag{62}$$

On the other hand, representing the first term in $G^{\delta}(v;a)$ in the form

$$\begin{aligned} \int_{\Omega} a|\nabla u|\mathrm{d}x &= \int_{\Omega}\left(\frac{a}{|\nabla v|}\right)^{1/2}|\nabla v|\cdot\left(\frac{a}{|\nabla v|}\right)^{1/2}|\nabla u|\mathrm{d}x \\ &\leqslant \left(\int_{\Omega}\frac{a}{|\nabla v|}|\nabla v|^2\mathrm{d}x\right)^{1/2}\cdot\left(\int_{\Omega}\frac{a}{|\nabla v|}|\nabla u|^2\mathrm{d}x\right)^{1/2} \\ &\leqslant \frac{1}{2}\int_{\Omega} a|\nabla v|\mathrm{d}x + \frac{1}{2}\int_{\Omega}\frac{a}{|\nabla v|}|\nabla u|^2\mathrm{d}x, \end{aligned}$$

we obtain

$$G^{\delta}(u;a) = \int_{\Omega} a|\nabla u|\mathrm{d}x + \frac{\delta}{2}\int_{\Omega}|\nabla(u-h)|^2\mathrm{d}x + \frac{1}{2}\int_{\partial\Omega} b(u-u_h)^2\mathrm{d}s$$
$$\leqslant \frac{1}{2}\int_{\Omega} a|\nabla v|\mathrm{d}x + J^{\delta}\left(u;\frac{a}{|\nabla v|}\right) \leqslant G^{\delta}(v;a). \tag{63}$$

The estimates (62) and (63) implies (61). □

Suppose now that the equality in (61) holds. Then the equality holds also in (62), in particular,

$$J^{\delta}\left(u;\frac{a}{|\nabla v|}\right) = J^{\delta}\left(v;\frac{a}{|\nabla v|}\right).$$

Thus v is also a global minimizer in $H^1(\Omega)$ of $J^{\delta}\left(\cdot;\frac{a}{|\nabla v|}\right)$. The uniqueness of the minimizer for J^{δ} yields $u = v$. □

7. The algorithm and reconstruction

In this section we present the algorithm and demonstrate its computational feasibility in numerical experiments.

For a given conductivity σ, the interior data was simulated by solving the forward problem subject to the complete electrode model (CEM) boundary conditions and setting

$$a_{\mathrm{CEM}} := \sigma|\nabla u|,$$

where u is the unique solution to (1) subject to (A.1)–(A.3) in the appendix. In solving the CEM problem we used the Galerkin finite element method.

The noisy data $\tilde{a}$ was obtained by adding to the exact coefficient a_{CEM} a normally distributed noise

$$\tilde{a} = a_{\mathrm{CEM}} + \Delta\cdot\frac{R}{||R||_2}, \tag{64}$$

where $\Delta > 0$ is the prescribed level of error, $R = R(0,1)$ is the normally distributed pseudo-random matrix with the zero mean and standard deviation one.

We also assume an *a priori* known upper bound for the conductivity

$$\sigma \leqslant \overline{\sigma}. \tag{65}$$

To solve the inverse problem, we use the iterative algorithm below, which produces a minimizing sequence based on successive applications of the result in theorem 3. At each step, a Robin problem is solved by the finite difference method (e.g. [29]), which is different from the method used to generate the data.

- **Initialization.** *Given $\tilde{a}, b, h, \Delta, \overline{\sigma}$, and a decreasing sequence $\delta_n \to 0^+$. Precompute the harmonic function u_h of trace h at the boundary, and set $\sigma_0 \equiv 1$.*
- **Step 1.** *Solve the problem*

$$\nabla\cdot(\sigma_0+\delta_1)\nabla u = 0 \text{ in } \Omega,$$
$$(\sigma_0+\delta_1)\frac{\partial u}{\partial\nu} = -bu + \delta_1\frac{\partial u_h}{\partial\nu} \text{ on } \partial\Omega$$

and let u_0 be its solution.

- **Step 2.** *Assume that the* $(k-1)$*st iteration was made. Update to*

$$\sigma_k = \min\left\{\frac{\tilde{a}}{|\nabla u_{k-1}|}, \overline{\sigma}\right\},$$

and solve the problem

$$\nabla \cdot (\sigma_k + \delta_{k+1})\nabla u = 0 \text{ in } \Omega,$$
$$(\sigma_k + \delta_{k+1})\frac{\partial u}{\partial \nu} = -bu + \delta_{k+1}\frac{\partial u_h}{\partial \nu} \text{ on } \partial\Omega.$$

Let u_k *be its solution.*

- **Step 3.** *Verify the stopping criteria*

$$\max ||\nabla u_k| - |\nabla u_{k-1}|| \leqslant \frac{\Delta}{\overline{\sigma}}$$

and

$$\frac{\|\sigma_k - \sigma_{k-1}\|_2}{\|\sigma_k\|_2} \leqslant TOL,$$

where TOL *is the tolerance level. If they are not satisfied, reassign the quantities for* $k-1 := k$ *and repeat Step 2.*

Otherwise, compute the approximate conductivity σ^δ *and interior voltage potential* u^δ *as*

$$\sigma^\delta = \sigma_k, \;\; u^\delta = u_k.$$

For the electrical conductivity σ we use an abdominal CT image (shown in the left upper corner in figure 1), which is scaled to the typical range $[1, 1.8]$ S m^{-1} of values of the electrical conductivity of biological tissues. The upper conductivity bound is set to $\overline{\sigma} = 2$ S m^{-1}. The electrodes are placed on the opposite sides of the unit square containing the image, so that the electrode supports are given by

$$e_- = \{(x_1, 0) : a \leqslant x_1 \leqslant b, 0 \leqslant a < 0, 0 < b \leqslant 1\}$$
$$e_+ = \{(x_1, 1) : a \leqslant x_1 \leqslant b, 0 \leqslant a < 0, 0 < b \leqslant 1\}.$$

The electrode aperture $b-a$ varies from 1 to few step sizes, and $-I_- = I_+ = 5 \cdot 10^{-3}$ A, $z = 8 \cdot 10^{-3}\,\Omega \cdot \mathrm{m}^2$.

Our method is able to image a minimum residue conductivity without any appeal to the voltage potential at the boundary (and it is the first of this kind). In addition to comparing the reconstructed conductivity with the exact one, we also compare it with the results that would be obtained by the iterative method of alternating split Bregman (ASB) type in [19], had the boundary values also been known. Originally introduced for finding common extrema of general convex functionals in [4], the application of ASB type algorithms to image analysis are far more recent, see [28]. The choice of the algorithm in [19] for comparison is motivated by its regularizing ability at singular points of the electric field (critical points of the voltage potential).

Since in the numerical experiments the simulated data $\tilde{a}$ is perturbed, we perform reconstructions for samples of 20 realizations of the perturbed interior data, so that a regularized solution is represented by the mean conductivity distribution. The relative errors of these means in the l_2-norm are computed. The regularization parameter is chosen as $\delta = C\Delta^{1/2}$, where $C = \text{const} > 0$.

Figure 1 aims to compare the original conductivity distribution (in the left upper corner) with the conductivity means recovered from the interior data $\tilde{a}$. The level of errors in $\tilde{a}$ is estimated as 10^{-5}, and $C = 1$ is chosen. In the upper row we show the conductivity means obtained from the interior data simulated for the full electrode aperture size. The conductivity mean obtained by the proposed iterative procedure is shown in the middle of the upper row. Its relative error is $4 \cdot 10^{-3}$, whereas the relative error of the conductivity mean obtained by the alternating split Bregman algorithm shown in the right upper corner is $1.5 \cdot 10^{-2}$. In the lower row we show the conductivity means for the reduced electrode aperture sizes: half aperture (the left corner), two step sizes $2h$ (the middle—the proposed algorithm, the right corner—the alternating split Bregman algorithm). The corresponding relative l_2-errors of reconstruction are $3 \cdot 10^{-3}$, $6 \cdot 10^{-3}$, and $3 \cdot 10^{-2}$, respectively.

Figure 2 demonstrates the performance of the proposed algorithm when recovering the conductivity from the simulated noisy interior data $\tilde{a}$. We set $C = 1$, $C = 2.5$, and $C = 3$, respectively, when choosing the regularization parameter. In the upper row we show the conductivity means for the full electrode aperture size and perturbed with the noise levels 10^{-3}, 10^{-2}, and $5 \cdot 10^{-2}$ (from left to right). The corresponding relative l_2-errors of reconstruction are $4.5 \cdot 10^{-3}$, $7.9 \cdot 10^{-3}$, and $4.3 \cdot 10^{-2}$. In the lower row we show the conductivity means recovered from the data $\tilde{a}$ simulated for the reduced electrode aperture sizes (in the left corner its size equals 1/2, in the middle—1/4, and in the right corner—$2h$) with the noise of the level 10^{-2} (from left to right). For all these configurations $C = 2.5$. The corresponding relative l_2-errors of reconstruction are $1.1 \cdot 10^{-2}$, $1.8 \cdot 10^{-2}$, and $5.3 \cdot 10^{-2}$, respectively.

Regardless of the method, the significant deterioration in quality of the reconstructed images (in the lower rows in both figures from left to right) is noted. This is due to the shrinking size of the electrode aperture, which yields a redistribution of equipotential lines with higher curvatures. In turn this effects the numerical computation of the gradient field used by the algorithms in the update step.

8. Conclusions

We demonstrate that it is possible to image the electrical conductivity using the magnitude of one current density field, without any voltage information at the boundary. The new method recovers an approximate conductivity within a given residual error. The method is based on solving a minimum weighted gradient problem corresponding to some Robin boundary conditions, which is further regularized to mitigate for the elliptic degeneracy present in the problem. A compactness property of the minimizing sequence is shown in the space of functions of bounded total variation. Numerical experiments are conducted to demonstrate the feasibility of the method, and they are also compared to one of the method that uses full knowledge of the voltage potential at the boundary.

Acknowledgment

The work of the second author is supported in part by the NSF grant DMS-1818882.

Appendix. On the equivalence between the Robin and complete electrode model (CEM)

We note here that, in the case of two electrodes the Robin and CEM boundary problems are equivalent up to a scaling factor. Not essential, but simplifying the exposition, we assume the the electrodes have equal surface areas, $|e| := |e_\pm|$. In the complete electrode model the voltage potential v solution of (1) inside Ω, and an unknown constant voltage V satisfy the boundary conditions

$$v + z\sigma\frac{\partial v}{\partial \nu} = \pm V, \quad \text{on } e_\pm, \tag{A.1}$$

$$\int_{e_\pm} \sigma\frac{\partial v}{\partial \nu}\mathrm{d}s = \pm I, \tag{A.2}$$

$$\frac{\partial v}{\partial \nu} = 0, \quad \text{on } \partial\Omega \setminus (e_+ \cup e_-). \tag{A.3}$$

Under the assumptions that Ω is a Lipschitz domain, σ is essentially bounded away from zero and infinity, the electrodes $e_\pm$ have positive impedance and are (relatively) open connected subsets of $\partial\Omega$ with disjoint closure, the CEM problem has a unique solution $(v; V) \in H^1(\Omega) \times R$, see [31], or the appendix in [26]. For an arbitrary $\lambda > 0$ the pair $(\lambda u_0, \lambda z I)$ clearly solves (1) and (A.1) (with $V = z\lambda I$), and (A.3). An application of Green's theorem in the Robin model yields $\int_{e_+} u_0 \mathrm{d}s = -\int_{e_-} u_0 \mathrm{d}s$, which well defines the scaling choice

$$\lambda^{-1} := \left(|e| - \frac{1}{zI}\int_{e_+} u_0 \mathrm{d}s\right) = \left(|e| + \frac{1}{zI}\int_{e_-} u_0 \mathrm{d}s\right).$$

With this choice of scaling, one can check that λu_0 also satisfies (A.2), and thus $\lambda u_0 = v$, and $a_0 = \lambda\sigma|\nabla v|$. Therefore, if we use to magnitude of the current density field corresponding to the Robin problem or to the CEM, we would recover the same conductivity $\sigma = a_0/|\nabla u_0| = |\sigma\nabla v|/|\nabla v|$.

References

[1] Bakushinsky A B and Goncharsky A V 1994 *Ill-Posed Problems: Theory and Applications* (Dordrecht: Kluwer)

[2] Bal G, Guo C and Monard F 2014 Imaging of anisotropic conductivities from current densities in two dimensions *SIAM J. Imaging Sci.* **7** 2538–57

[3] Bal G, Guo C and Monard F 2014 Inverse anisotropic conductivity from internal current densities *Inverse Problems* **30** 025001

[4] Bregman L 1967 The relaxation method of finding the common points of convex sets and its application to the solution of problems of convex optimization *USSR Comput. Math. Math. Phys.* **7** 200–17

[5] Fortin M and Glowinski R 1983 *Augmented Lagrangian Methods: Applications to the Numerical Solution of Boundary Value Problems* (Amsterdam: Elsevier) vol 15

[6] Giusti E 1984 *Minimal Surfaces and Functions of Bounded Variations* (Boston, MA: Birkhäuser)

[7] Hoell N, Moradifam A and Nachman A 2014 Current density impedance imaging with an anisotropic conductivity in a known conformal class *SIAM J. Math. Anal.* **46** 3969–90

[8] Jerrard R L, Moradifam A and Nachman A I 2018 Existence and uniqueness of minimizers of general least gradient problems *J. Reine Angew. Math.* **734** 71–97

[9] Lions J-L and Magenes E 1972 *Non-Homogeneous Boundary Value Problems and Applications* vol I (Berlin: Springer)
[10] Ma J *et al* 2013 Experimental implementation of a new method of imaging anisotropic electric conductivities *Proc. EMBC* pp 6437–40
[11] Joy M J *et al* 2004 A new approach to current density impedance imaging (CDII) *Proc. ISMRM (Kyoto, Japan)*
[12] Kim S *et al* 2002 On a nonlinear partial differential equation arising in magnetic resonance electrical impedance tomography *SIAM J. Math. Anal.* **34** 511–26
[13] Kim Y-J and Lee M-G 2015 Well-posedness of the conductivity reconstruction from an interior current density in terms of Schauder theory *Q. Appl. Math.* **73** 419–33
[14] Kwon O *et al* 2002 Magnetic resonance electric impedance tomography (MREIT): simulation study of J-substitution algorithm *IEEE Trans. Biomed. Eng.* **49** 160–7
[15] Kwon O, Lee J Y and Yoon J R 2002 Equipotential line method for magnetic resonance electrical impedance tomography *Inverse Problems* **18** 1089–100
[16] Lee J Y 2004 A reconstruction formula and uniqueness of conductivity in MREIT using two internal current distributions *Inverse Problems* **20** 847–58
[17] Montalto C and Stefanov P 2013 Stability of coupled physics inverse problems with one internal measurement *Inverse Problems* **29** 125004
[18] Montalto C and Tamasan A 2017 Stability in conductivity imaging from partial measurements of one interior current *Inverse Problems Imaging* **11** 339–53
[19] Moradifam A, Nachman A and Timonov A 2012 Convergent algorithm for the hybrid problem of reconstructing conductivity from minimal interior data *Inverse Problems* **28** 084003
[20] Moradifam A, Nachman A and Tamasan A 2012 Conductivity imaging from one interior measurement in the presence of perfectly conducting and insulating inclusions *SIAM J. Math. Anal.* **44** 3969–90
[21] Moradifam A, Nachman A and Tamasan A 2018 Uniqueness of minimizers of weighted least gradient problems arising in conductivity imaging *Calculus Variations PDE* **57** 6
[22] Nachman A, Tamasan A and Timonov A 2007 Conductivity imaging with a single measurement of boundary and interior data *Inverse Problems* **23** 2551–63
[23] Nachman A, Tamasan A and Timonov A 2009 Recovering the conductivity from a single measurement of interior data *Inverse Problems* **25** 035014
[24] Nachman A, Tamasan A and Timonov A 2010 Reconstruction of planar conductivities in subdomains from incomplete data *SIAM J. Appl. Math.* **70** 3342–62
[25] Nachman A, Tamasan A and Timonov A 2011 Current density impedance imaging, tomography and inverse transport theory *AMS Contemp. Math.* **559** 135–50
[26] Nachman A, Tamasan A and Veras J 2016 A weighted minimum gradient problem with complete electrode model boundary conditions for conductivity imaging *SIAM J. Appl. Math.* **76** 1321–43
[27] Nashed M Z and Tamasan A 2010 Structural stability in a minimization problem and applications to conductivity imaging *Inverse Problems Imaging* **5** 219–36
[28] Osher S *et al* 2005 An iterative regularization method for total variation-based image restoration *Multiscale Model. Simul.* **4** 460–89
[29] Samarskii A A 2001 *The Theory of Difference Schemes* (New York: Marcell Decker Inc.)
[30] Scott G C *et al* 1991 Measurement of nonuniform current density by magnetic resonance *IEEE Trans. Med. Imaging* **10** 362–74
[31] Somersalo E, Cheney M and Isaacson D 1992 Existence and uniqueness for electrode models for electric current computed tomography *SIAM J. Appl. Math.* **54** 1023–40
[32] Tamasan A and Veras J 2012 Conductivity imaging by the method of characteristics in the 1-Laplacian *Inverse Problems* **28** 084006
[33] Tamasan A, Timonov A and Veras J 2014 Stable reconstruction of regular 1-Harmonic maps with a given trace at the boundary *Appl. Anal.* (https://doi.org/10.1080/00036811.2014.918260)
[34] Vauhkonen P *et al* 1999 Three-dimensional electrical impedance tomography based on the complete electrode model *IEEE Trans. Biomed. Eng.* **46** 1150–60
[35] Zhang N 1992 Electrical impedance tomography based on current density imaging *MSc Thesis* University of Toronto, Canada
[36] Ziemer W P 1969 *Weakly Differentiable Functions* (New York: Springer)